Metabolism 133 (2022) 155240

Contents lists available at ScienceDirect

Metabolism

journal homepage: www.journals.elsevier.com/metabolism

TCF7L2 plays a complex role in human adipose progenitor biology, which might contribute to genetic susceptibility to type 2 diabetes

Manu Verma [a], Nellie Y. Loh [a], Rugivan Sabaratnam [a,b,c], Senthil K. Vasan [a], Andrea D. van Dam [a], Marijana Todorčević [a], Matthew J. Neville [a], Enrique Toledo [d], Fredrik Karpe [a,e], Constantinos Christodoulides [a,e,*]

[a] Oxford Centre for Diabetes, Endocrinology and Metabolism, Radcliffe Department of Medicine, University of Oxford, Oxford OX3 7LE, UK
[b] Steno Diabetes Center Odense, Odense University Hospital, DK-5000 Odense, Denmark
[c] Department of Clinical Research, University of Southern Denmark, DK-5000 Odense, Denmark
[d] Department of Computational Biology, Novo Nordisk Research Centre Oxford, UK
[e] NIHR Oxford Biomedical Research Centre, OUH Foundation Trust, Oxford OX3 7LE, UK

ARTICLE INFO

Keywords:
TCF7L2
Adipose
Adipogenesis
Type 2 diabetes
WNT
Human

ABSTRACT

Introduction: Non-coding genetic variation at *TCF7L2* is the strongest genetic determinant of type 2 diabetes (T2D) risk in humans. TCF7L2 encodes a transcription factor mediating the nuclear effects of WNT signaling in adipose tissue (AT). *In vivo* studies in transgenic mice have highlighted important roles for TCF7L2 in adipose tissue biology and systemic metabolism.
Objective: To map the expression of *TCF7L2* in human AT, examine its role in human adipose cell biology *in vitro*, and investigate the effects of the fine-mapped T2D-risk allele at rs7903146 on AT morphology and TCF7L2 expression.
Methods: Ex vivo gene expression studies of *TCF7L2* in whole and fractionated human AT. *In vitro* TCF7L2 gain- and/or loss-of-function studies in primary and immortalized human adipose progenitor cells (APCs) and mature adipocytes (mADs). AT phenotyping of rs7903146 T2D-risk variant carriers and matched controls.
Results: Adipose progenitors (APs) exhibited the highest *TCF7L2* mRNA abundance compared to mature adipocytes and adipose-derived endothelial cells. Obesity was associated with reduced *TCF7L2* transcript levels in whole subcutaneous abdominal AT but paradoxically increased expression in APs. In functional studies, TCF7L2 knockdown (KD) in abdominal APs led to dose-dependent activation of WNT/β-catenin signaling, impaired proliferation and dose-dependent effects on adipogenesis. Whilst partial KD enhanced adipocyte differentiation, near-total KD impaired lipid accumulation and adipogenic gene expression. Over-expression of TCF7L2 accelerated adipogenesis. In contrast, TCF7L2-KD in gluteal APs dose-dependently enhanced lipid accumulation. Transcriptome-wide profiling revealed that TCF7L2 might modulate multiple aspects of AP biology including extracellular matrix secretion, immune signaling and apoptosis. The T2D-risk allele at rs7903146 was associated with reduced AP TCF7L2 expression and enhanced AT insulin sensitivity.
Conclusions: TCF7L2 plays a complex role in AP biology and has both dose- and depot-dependent effects on adipogenesis. In addition to regulating pancreatic insulin secretion, genetic variation at *TCF7L2* might also influence T2D risk by modulating AP function.

1. Introduction

Adipose tissue (AT) plays a central role in the control of whole-body energy homoeostasis. Firstly, it provides a safe depot for excess calorie storage as triglycerides, thereby protecting extra-adipose tissues from lipotoxicity [1]. Secondly, it releases energy as free fatty acids (FFAs) during periods of energy demand such as fasting and exercise. Finally, it directly regulates systemic energy balance and insulin sensitivity *e.g.*, through the secretion of hormones such as leptin and adiponectin [2]. AT expands through an increase in adipocyte number (hyperplasia) and/or size (hypertrophy). Hyperplastic AT growth is mediated through the generation of new adipocytes from adipose progenitors (APs), namely

* Corresponding author at: Oxford Centre for Diabetes, Endocrinology and Metabolism, Churchill Hospital, Oxford OX3 7LE, UK.
E-mail address: costas.christodoulides@ocdem.ox.ac.uk (C. Christodoulides).

https://doi.org/10.1016/j.metabol.2022.155240
Received 26 October 2021; Accepted 4 June 2022
Available online 10 June 2022

adipose stem cells and preadipocytes, and is associated with enhanced systemic insulin sensitivity and improved glucose and lipid metabolism. In contrast, adipocyte hypertrophy results in AT fibrosis and inflammation, which promote the development of insulin resistance [3,4].

WNTs are a family of secreted growth factors functioning in autocrine and paracrine fashions to regulate stem cell biology *via* multiple downstream signaling cascades [5–7]. In the best-characterized, canonical pathway, WNT binding to their receptor complex leads to nuclear accumulation of the transcriptional co-activator β-catenin, which interacts with TCF/LEF transcription factors to activate the expression of WNT target genes. There are four mammalian TCF/LEF family members, TCF7, TCF7L1, TCF7L2 and LEF1 [8], with TCF7L1 and TCF7L2 exhibiting the highest AT expression [9]. According to the prevailing model, in the absence of WNTs, TCF/LEF proteins are bound to transcriptional co-repressors and suppress WNT/β-catenin signaling. However, the transcriptional switch promoted by WNTs might also involve an exchange of TCF/LEF family members, with TCF7L1 generally acting as a repressor of WNT target genes, LEF1 and TCF7 as activators, and TCF7L2 having both repressor and activator functions, depending on cellular context [8,10,11].

Work from the MacDougald laboratory first highlighted a potential role for TCF/LEFs in AT biology. Specifically, a dominant negative TCF7L2 mutant, lacking its β-catenin binding domain, was shown to promote spontaneous adipogenesis of 3T3-L1 preadipocytes and trans-differentiation of C2C12 myoblasts to adipocytes [12,13]. Recently, the specific role of TCF7L2 in *in vitro* adipogenesis was investigated with conflicting results. Whilst Chen et al. showed that TCF7L2 knockdown (KD) in 3T3-L1 preadipocytes leads to impaired adipocyte differentiation [14] in another study, TCF7L2 deletion in immortalized inguinal mouse APs resulted in enhanced adipogenesis [15]. *In vivo*, adipose expression of *Tcf7l2* was suppressed by high-fat diet (HFD)-induced and genetic obesity [15,16]. Homozygous global *Tcf7l2* null mice died perinatally whilst heterozygous null animals were lean and had enhanced glucose tolerance and insulin sensitivity compared to wild-type controls [17,18]. Conversely, transgenic mice with global over-expression of *Tcf7l2*, displayed HFD-induced glucose intolerance [18], which was driven by *Tcf7l2* over-expression in non-pancreatic tissues [19]. Contrasting these findings, targeted deletion of *Tcf7l2* in mature adipocytes (mADs) resulted in increased adiposity, hyperinsulinemia and/or glucose intolerance [14,15,20]. In humans, *TCF7L2* expression was decreased in the subcutaneous abdominal (hereafter abdominal) AT of subjects with impaired glucose tolerance [14] or reduced systemic insulin sensitivity [21]. Notably, non-coding genetic variation at *TCF7L2* was shown to be the strongest genetic determinant of T2D risk in Europeans [22,23]. The same signal was also associated with fat distribution [24] and sex-specific differences in plasma FFA responses to an oral glucose tolerance test [25]. Motivated by these findings we investigated the largely unexplored role of TCF7L2 in human AT biology.

2. Materials and methods

2.1. Study population

Study volunteers were recruited from the Oxford Biobank (OBB), a population-based cohort of healthy 30–50-year-old subjects [26]. Paired abdominal and visceral biopsies were collected from patients undergoing elective surgery as part of the MolSURG study [27]. Plasma biochemistry [26] and adipocyte sizing [27] were undertaken as described. All studies were approved by the Oxfordshire Clinical Research Ethics Committee and all volunteers gave written, informed consent.

2.2. Cell culture

AT biopsy-derived primary or immortalized APs were cultured and differentiated as described [28,29]. Primary endothelial cells were isolated using a CD31 MicroBead Kit (Miltenyi Biotec). Intracellular lipid quantification was undertaken using AdipoRed (Lonza) and a multi-well plate reader (PerSeptive Biosystems, Perkin Elmer).

2.3. Generation of de-differentiated fat (DFAT) cells

DFAT cells were generated by selection and de-differentiation of lipid-laden, *in vitro* differentiated immortalized APs with modifications [27] (see Supplemental information).

2.4. Lentiviral constructs and generation of stable AP lines

TCF7L2 (sh843, TRCN0000262843; sh897, TRCN0000061897; sh444, TRCN0000282444; sh848, TRCN0000262848) and control (scrambled) shRNA plasmid vectors were purchased (Sigma-Aldrich). The TOPflash reporter vector [30] was a gift from Roel Nusse (Addgene #24307). Lentiviral particles were produced in HEK293 cells using MISSION® (Sigma-Aldrich) packaging mix. Stable AP lines were generated by transduction of cells with lentiviral particles and selected using (2 μg/ml) puromycin.

2.5. Doxycycline-inducible AP lines

The *TCF7L2* sequence (from TCF4E pcDNA3, a gift from Frank McCormick, Addgene #32738) [31] was cloned into the pCW57.1 lentiviral vector (gift from David Root, Addgene plasmid #41393) and oligonucleotides for sh843 were cloned into tet-pLKO-puro doxycycline-inducible expression lentiviral vector (gift from Dmitri Wiederschain, Addgene #21915) [32] for inducible TCF7L2 over-expression and KD respectively. Stable doxycycline-inducible AP lines were generated by transduction of cells with lentiviral particles and selected using (2 μg/ml) puromycin.

2.6. siRNA mediated TCF7 KD in DFAT AP lines

Control (ON-TARGETplus Non-targeting Pool, #D-001810-10-05) and TCF7 (ON-TARGETplus Human TCF7 (6932), SMARTpool, #L-019735-00-0005) siRNAs were purchased from Horizon Discovery Ltd (Cambridge, UK). Abdo shCN and sh843 DFAT APs seeded in 12-well plates were transfected with 0.1 nM siRNAs using Lipofectamine RNAiMAX transfection reagent (ThermoFisher Scientific), according to manufacturer's instructions. 48 h post-transfection, cells were harvested for RNA, or differentiated in standard adipocyte differentiation media.

2.7. CRISPR genome editing

Stable hCas9 expressing DFAT APs were generated by transduction of lentiCas9-EGFP (gift from Phil Sharp & Feng Zhang, Addgene plasmid #63592) [33] or pLV-[Exp]-CAG>hCas9:P2A:Bsd vector (Vectorbuilder) followed by selection using EGFP or blasticidin (2 μg/ml) respectively. Prior to this, DFAT APs were immortalized and de-differentiated as described apart from using Hygromycin (100 μg/ml) for selection.

For base editing, clonal lines with the highest EGFP expression (hCas9) were selected using FACS and expanded. Transfection of two sets of single stranded oligonucleotide donors (ssODNs) (CTTTTTAGATATTATATAATTTAATTGCCGTATGAGGCACCCTTAGTTTTCAGACGAGAAAC, GTTTCTCGTCTGAAAACTAAGGGTGCCTCATACGGCAATTAAATTATATAATATCTAAAA) & sgRNAs (TATAATTTAATTGCCGTATGAGG, AAAACTAAGGGTGCCTCATACGG) (IDT, UK) was undertaken using Neon Transfection system (ThermoFischer, UK) following manufacturer's instructions for RNP electroporation (IDT, UK). Validation of CRISPR editing was done on pooled cells post transfection using Sanger sequencing and TIDE analysis [34]. Single cell cloning of sham treated or edited clones was undertaken *via* FACS followed by colony expansion.

For loss of function, stable TCF7L2 KD DFAT APs were generated by

lentiviral transduction of sgRNAs (#28 – CGGCCATCAACCAGATCCTT, #296 – TGGGCGAGAGCGATCCGTTG, VectorBuilder) against TCF7L2 and selected using puromycin (2 μg/ml).

2.8. Pharmacological inhibitors

KYA1791K potassium salt (WNT/β-catenin inhibitor; #SML1831) and the JAK Inhibitor I (#420099) were purchased from (Merck Life Science UK Ltd). To study the effects of KYA1797K treatment on adipogenesis, shCN and sh843 Abdo DFAT APs were seeded at a density of 14K/well in a 96-well plate. Two days later, cells were differentiated in the presence of 0.1 μM, 1 μM or 2.5 μM KYA1797K, or vehicle (DMSO) for 14 days. Intracellular lipid accumulation was quantified as a metric for adipogenesis using AdipoRED. To assess TOPflash activity, shCN and sh843 Abdo DFAT APs (harboring TOPFlash reporter) were seeded in 96-well plates were treated with indicated concentrations of KYA1797K or vehicle (DMSO) in growth media for 48 h, then assessed using the Luciferase Assay System (Promega). Luciferase activity was normalized to mCherry fluorescence.

2.9. Proliferation assays

Equal number of APs were seeded, trypsinised and counted using a Cellometer Auto T4 (Nexcelom Bioscience) every 96 h or using CyQUANT™ cell proliferation assays. Doubling time was calculated using the formula: $T_d = (t_2 - t_1) \times [\log(2) \div \log(q_2 \div q_1)]$, where t = time (days), q = cell number.

2.10. Luciferase assays

To assess *cis*-regulatory activity, a 151 base pair genomic sequence centred around rs7903146 was cloned into a luciferase reporter vector (pGL4.23[luc2/minP], Promega) and co-transfected with pRL-SV40 (Promega) into HEK293 (Lipofectamine 2000, Thermo Fisher Scientific) or DFAT cells (Neon Transfection System, Thermo Fisher Scientific). 48 h post-transfection, luciferase activity was assessed using the Dual-Luciferase® Reporter Assay System (Promega) on Veritas Microplate Luminometer (Turner Biosystems).

2.11. TOPflash reporter assays

β-Catenin transcriptional activity in TCF7L2-KD DFAT cells was determined as described [28].

2.12. Glucose uptake assay

In vitro differentiated DFAT APs were incubated in basal medium containing either vehicle or 0.05 μg/ml doxycycline (to induce TCF7L2 KD) for 48 h. Basal and insulin stimulated (25 nM insulin, 30 min, 37 °C & 5 % CO_2) glucose uptake assay was performed as described [27].

2.13. Real time-PCR and western blots

qRT-PCR and western blotting were performed using TaqMan assays and standard protocols (see Supplemental information).

2.14. RNA sequencing, pathway enrichment and transcription factor clustering analysis

RNA sequencing (RNA-Seq) was performed in scrambled control, sh897 and sh843 TCF7L2-KD DFAT abdominal APs and primary abdominal and gluteal APs (see Supplemental information). Briefly, differentially regulated genes (DEGs) (false discovery rate <0.05) were selected for further analysis. Pathway enrichment was done using ClusterProfiler R package [35] and transcription factor clustering was undertaken as previously reported [36].

2.15. Statistical analysis

Statistical analysis was performed using R, SPSS, Stata or GraphPad. For parametric data, Pearson correlation, linear regression analysis, two-tailed Student's test with Welch's correction (where appropriate) for 2 groups, or one- or two-way ANOVA followed by appropriate *post hoc* tests for multiple groups were used. For non-parametric data, Spearman's correlation, Wilcoxon matched-pairs signed rank test or Kruskal-Wallis test followed by Dunn's multiple comparisons test were used. Smoothened splines using generalized additive models were used to investigate the relationship between adipose tissue insulin resistance (fasting insulin*FFAs) and body mass index (BMI) in different rs7903146 genotype carriers. P-values were corrected for multiple comparisons or where appropriate age, BMI, and sex. $P < 0.05$ was considered significant.

3. Results

3.1. TCF7L2 expression is highest in APs

To elucidate the function of TCF7L2 in human AT we first mapped its adipose expression profile. *TCF7L2* mRNA abundance tended to be higher in abdominal *versus* gluteal AT ($P = 0.05$) (Fig. 1A) but did not differ between the abdominal and omental depots (Fig. 1B). Compared to obese subjects, lean individuals had higher *TCF7L2* expression in abdominal AT (Fig. 1A). In fractionated AT, *TCF7L2* transcript levels were higher in cultured APs than mADs (Fig. 1C) and adipose-derived endothelial cells from both the abdominal and gluteal depots (Fig. 1D). Of note, the expression of adipose stem cell and preadipocyte marker genes, as previously defined in single cell RNA-Seq studies of the stromal vascular fraction of human AT, was enriched in the cultured AP cells (Fig. S1) [37,38]. Finally, *TCF7L2* mRNA abundance in abdominal APs correlated positively with BMI whilst a directionally opposite trend was detected for abdominal mADs (Fig. 1E, F). No associations between *TCF7L2* expression in gluteal adipose cell fractions and BMI were detected (Fig. S2). Based on these data we focused on deciphering the function of TCF7L2 in APs.

3.2. TCF7L2 dose-dependently modulates AP differentiation

We investigated the role of TCF7L2 in AP biology using immortalized DFAT cells [27]. These retain their depot of origin gene expression signatures (Fig. S3) and have a high adipogenic capacity. Stable TCF7L2-KD in these cells was achieved with two independent shRNAs targeting the universal exon 9 of *TCF7L2* (Fig. 2A, B). The first shRNA (sh897) led to 30 % and 68 % TCF7L2-KD at mRNA and protein level, respectively whilst the second shRNA (sh843), led to 70 % reduction in *TCF7L2* expression and 99 % TCF7L2 protein KD. Both partial and near-total TCF7L2-KD led to impaired AP proliferation (Fig. 2C). Partial TCF7L2-KD was also associated with enhanced adipogenesis as determined by increased lipid accumulation and elevated adipogenic gene expression (Fig. 2D-H). In marked contrast, near-total TCF7L2-KD resulted in impaired adipogenesis. These findings were replicated in primary abdominal TCF7L2-KD cells from two independent subjects (Fig. 2I, J). Furthermore, bioinformatic analyses did not identify any confounding off-target effects on gene expression associated with either shRNA (Table S1). The dose-dependent effects of TCF7L2-KD on adipogenesis were also confirmed with a separate pair of shRNAs (Fig. S4), and TCF7L2 knockout using CRIPSR/Cas9 (Fig. S4D–F). We also explored the role of TCF7L2 in adipogenesis in gluteal DFAT cells. Stable TCF7L2-KD using sh897 and sh843 also dose-dependently modulated gluteal adipocyte differentiation. However, in sharp contrast to findings in abdominal APs, near-total TCF7L2-KD in gluteal cells led to enhanced adipogenesis as determined by increased lipid accumulation (Fig. S4G–I). A similar but less pronounced pro-adipogenic trend was also detected in partial TCF7L2-KD gluteal APs (Fig. S4G–I). In

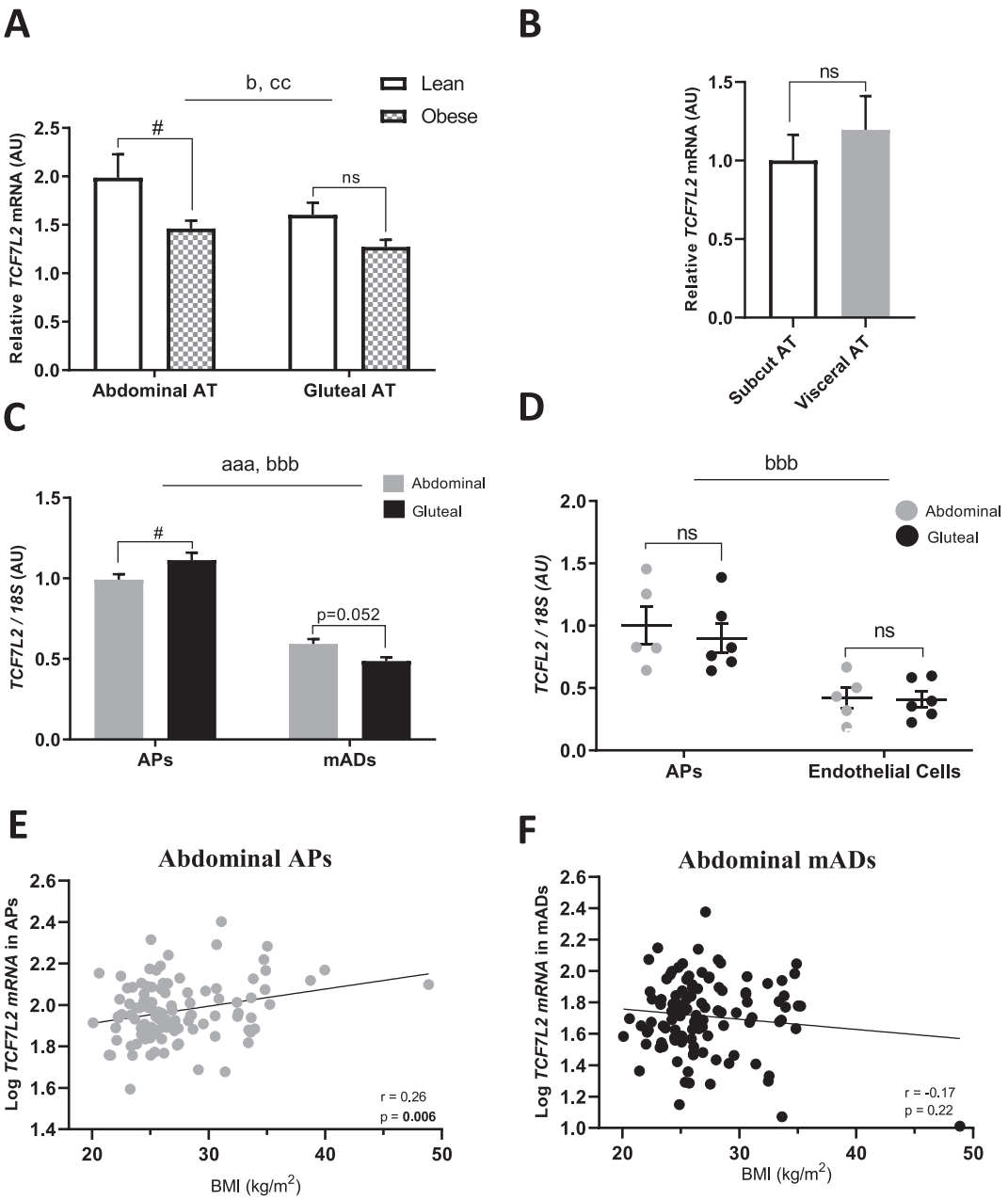

Fig. 1. *Ex vivo TCF7L2* expression in human adipose depots and adipose cell fractions. *TCF7L2* expression in paired samples of (A) subcutaneous (SC) abdominal and gluteal adipose tissue (AT) biopsies from lean and obese subjects (n = 30 [15F]/group; Lean – Age 43.9 ± 4.7 years, BMI 22.0 ± 1.1 kg/m^2; Obese – Age 43.9 ± 3.6 years, BMI 34.5 ± 2.4 kg/m^2). Data analysed by two-way ANOVA (Depot * Lean/Obese p = ns, ^{b}Abdo *vs.* Glut P = 0.051, ^{cc}Lean *vs.* Obese P < 0.01) followed by Šídák's multiple comparisons test $^{\#}$P < 0.05. (B) Abdominal SC and visceral AT biopsies (n = 27 [16F]/group; age - 59.1 ± 11.8 years, BMI - 28.2 ± 7.2 kg/m^2). Data analysed by unpaired *t*-test with Welch's correction. (C) Cultured APs and mature adipocytes (mADs) from SC abdominal and gluteal AT biopsies (n = 108–114 [59F]/group; age - 45.3 ± 8.7 years, BMI - 27.2 ± 4.5 kg/m^2). Data analysed by two-way ANOVA (^{aaa}Cell type * Depot P < 0.001, ^{bbb}Cell type p < 0.001, Depot P = ns) followed by Šídák's multiple comparisons test $^{\#}$P < 0.05. (D) Cultured APs and adipose-derived endothelial cells from SC abdominal and gluteal AT biopsies (n = 5–6 [5-6F]/group; age - 51.9 ± 7.9 years, BMI - 28.8 ± 4.0 kg/m^2). Data analysed by two-way ANOVA (Cell type * Depot p = ns, ^{bbb}Cell type P < 0.001, Depot p = ns) followed by Šídák's multiple comparisons test. Error bars are means ± SEM. (E, F) Pearson correlations between *TCF7L2* expression in cultured APs and mADs from SC abdominal AT biopsies and donor BMI (n = 110–113 [59F]/group; age - 45.3 ± 8.7 years, BMI - 27.2 ± 4.5 kg/m^2). Slope is plotted using simple linear regression. qRT-PCR data were normalized to geometric mean of (A) *PPIA*, *PGK1*, *PSMB6*, and *IPO8*, (B) *PPIA* and *PGK1*, or (C–F) to 18S rRNA levels. $^{\#}$P < 0.05 (adjusted for multiple comparisons). Histograms are means ± SEM. Age and BMI data are means ± SEM.

complimentary experiments we examined the effects of inducible over-expression of the *TCF7L2* isoform (ENST00000369397.8) with the highest subcutaneous AT expression (https://gtexportal.org) in abdominal AP function using a Tet-On system (Fig. 3). The doxycycline dose was selected to induce 2- and 5-fold baseline *TCF7L2* over-expression compared to vehicle treated APs transduced with the same vector, which corresponded to an equivalent increase in protein production (and 2.6 and 6.6-fold higher protein production *versus* vehicle treated empty vector controls) (Fig. 3A, B). Neither low- nor high-dose *TCF7L2* over-expression modulated AP proliferation (Fig. 3C). On the other hand, 2-fold *TCF7L2* over-expression tended to inhibit lipid accumulation (treatment by genotype interaction test P = 0.051) but did not suppress adipogenic gene expression (Figs. S5B & S6). However, the doxycycline-induced increase in *TCF7L2* mRNA abundance was not

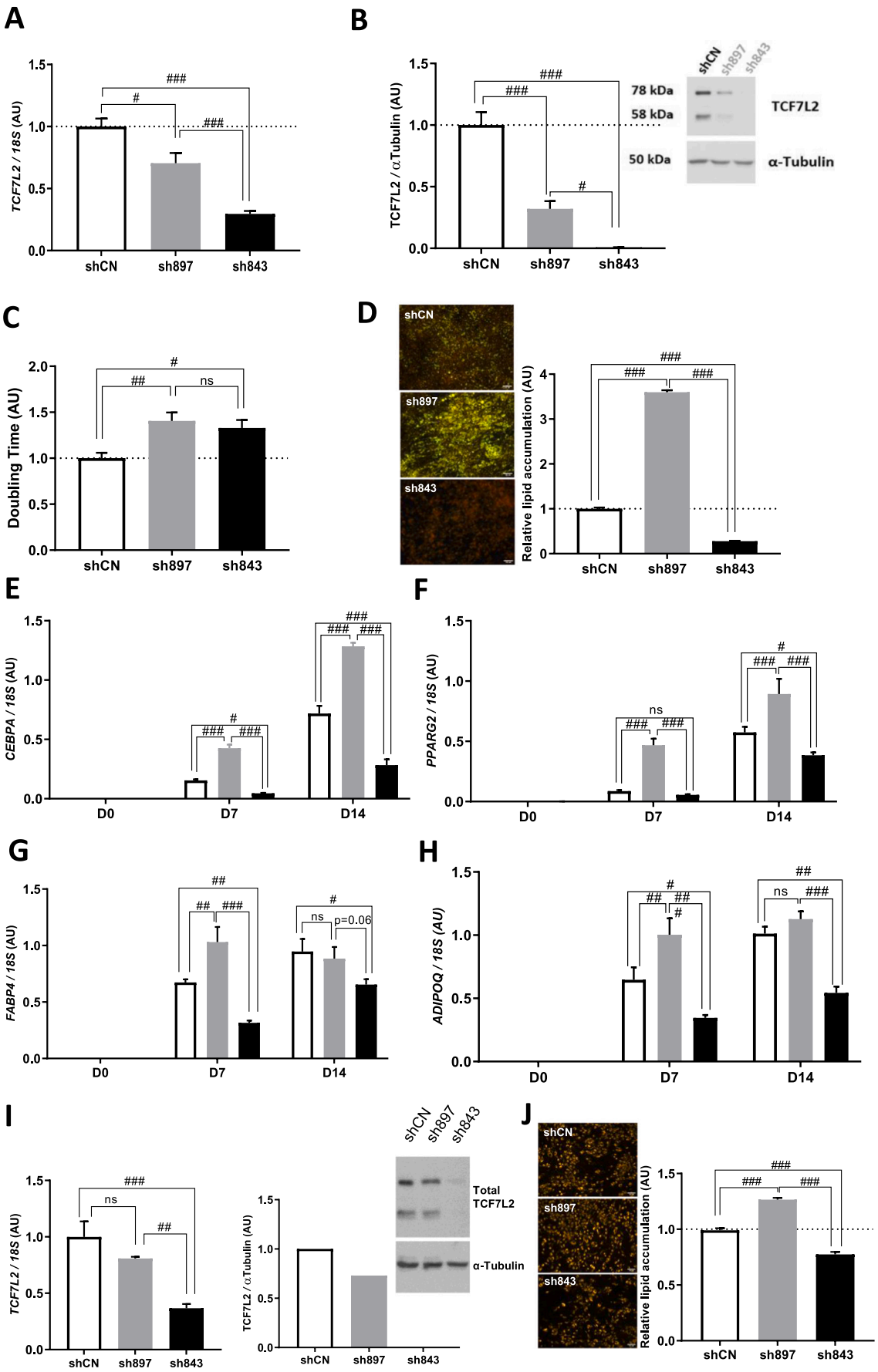

(caption on next page)

Fig. 2. TCF7L2 KD in abdominal APs impairs proliferation and dose-dependently regulates differentiation. (A–H) TCF7L2 KD in DFAT abdominal APs. shCN = scrambled control, sh897 = moderate and sh843 = high TCF7L2-KD DFAT abdominal APs. TCF7L2 KD was confirmed by (A) qRT-PCR and (B) western blot in DFAT abdominal APs. (C) Doubling time of control, sh897 and sh843 TCF7L2-KD APs. (D) Representative micrographs of control, sh897 and sh843 APs at day 14 of adipogenic differentiation (scale bar 100 μM). The histogram shows the relative lipid accumulation (as a marker for differentiation) assessed by AdipoRed lipid stain (n = 24 wells/group) (E–H) Relative mRNA levels of adipogenic genes *CEBPA*, *PPARG2*, *FABP4* and *ADIPOQ* at baseline (day 0), day 7 and day 14 of adipogenic differentiation. (I–J) TCF7L2 KD in human primary abdominal APs (n = 2 subjects [0F]; mean age = 45.5. Mean BMI = 29.12; rs7903146 genotype [CC]). (I) Confirmation of TCF7L2 KD by qRT-PCR and western blot in human primary abdominal APs (western blots from one experiment). (J) Representative micrographs of control, moderate (sh897) and high (sh843) TCF7L2-KD human primary abdominal APs at day 14 of adipogenic differentiation (scale bar 100 μM). The histogram shows the relative lipid accumulation, assessed by AdipoRed (n = 16 wells/group). (A-D, I, J) Data analysed by one-way ANOVA followed by Tukey's multiple comparisons test. (E–H) Data analysed by two-way ANOVA followed by Tukey's multiple comparisons test. $^{###}P < 0.001$, $^{##}P < 0.01$, $^{#}P < 0.05$ (adjusted for multiple comparisons). Histograms are means ± SEM. Data obtained from 3 independent experiments. qRT-PCR data were normalized to 18S rRNA levels. α-Tubulin was used as a loading control for western blots.

sustained throughout differentiation (Figs. 3A, B, S5C, D). In contrast, 5-fold *TCF7L2* over-expression accelerated adipogenesis (Figs. 3D–H & S7). We conclude that, at least endogenously expressed TCF7L2 has dose-dependent actions on adipogenesis *in vitro*.

3.3. TCF7L2 dose-dependently modulates WNT/β-catenin signaling in APs

We investigated whether the effects of TCF7L2 on abdominal AP biology were driven by altered WNT/β-catenin signaling. Only near-total TCF7L2-KD led to increased expression of the universal WNT target gene *AXIN2* (Fig. 4A). Using TCF7L2-KD cells stably expressing the TOPflash promoter reporter, which monitors β-catenin transcriptional activity, we confirmed that near-total TCF7L2-KD was associated with robust WNT signaling activation whilst more modest activation was also detected following partial KD both in the absence and presence of WNT3A (Fig. 4B). Interestingly, despite increased β-catenin transcriptional activity, active β-catenin protein levels were decreased in both partial and near-total TCF7L2-KD cells (Fig. 4C). We also examined the expression of other TCF/LEF family members in TCF7L2-KD abdominal APs (Figs. 4D, E & S8A, B). Only *TCF7* and *TCF7L1* were expressed in these cells. Notably, high-efficiency TCF7L2-KD resulted in increased TCF7 mRNA and protein abundance in both DFAT and primary abdominal APs (Fig. 4D, E). Collectively these findings indicate that TCF7L2 functions to antagonize WNT/β-catenin signaling in abdominal APs. However, chemical inhibition of this pathway with KYA1797K [39] (Fig. S9), which targets β-catenin for proteosomal degradation or *transient* siRNA KD of TCF7 failed to rescue adipogenesis in high-efficiency TCF7L2-KD cells (Fig. S10).

3.4. Transcriptome-wide profiling reveals that TCF7L2 regulates multiple aspects of AP biology

To identify the genes and biological processes regulated by TCF7L2 in APs, we undertook RNA sequencing of abdominal TCF7L2-KD cells (Fig. 5A). Near-total and partial TCF7L2-KD altered the expression of 7470 and 3921 genes respectively (Fig. 5B). Equal numbers of genes (50 %) were up- and down-regulated following near-total TCF7L2-KD, which was associated with increased *TCF7* expression. In contrast, partial TCF7L2-KD led to a higher proportion of up-regulated genes (54 %). In fact, only three of the top 30 differentially expressed genes were down-regulated in partial TCF7L2-KD cells (Fig. 5C, D) highlighting that TCF7L2 primarily functions as a transcriptional repressor in abdominal APs. Gene ontology (GO) analysis revealed that the cluster of genes suppressed in high-efficiency TCF7L2-KD cells was enriched for pathways and processes involved in cell cycle, glycolysis, p53 signaling and ribosome biogenesis (Fig. 5E). Interestingly, the cell cycle and ribosome biogenesis pathways were previously shown to be transcriptionally positively regulated by WNT/β-catenin signaling [40]. Accordingly, the expression of many β-catenin targets was reduced in high-efficiency TCF7L2-KD APs (Fig. S11) (see Discussion for clarification of this paradox). The cluster of up-regulated genes in near-total TCF7L2-KD cells was enriched for genes involved in interferon signaling, extracellular matrix (ECM) organization, and mesenchymal cell differentiation. In partial TCF7L2-KD cells the down-regulated gene set was also enriched for the GO annotations cell cycle, glycolysis and p53 signaling whilst the up-regulated gene cluster was enriched for genes involved in interferon signaling, ECM organization, and neutrophil activation (Fig. 5E). Given that both interferon alpha [41] and gamma [42] were shown to suppress adipogenesis *via* JAK/STAT signaling and that a non-selective JAK inhibitor rescued this phenotype [41,42], we tried unsuccessfully to rescue adipocyte differentiation in high-efficiency TCF7L2-KD cells using the same agent (Fig. S12). We also searched for transcription factors acting in concert with TCF7L2 to regulate the adipogenic potential of abdominal APs. To do this, we manually curated a set of transcription factors previously shown to modulate adipogenesis [43,44] and investigated which of these factors regulated, in a cell-type agnostic manner, the same group of target genes as TCF7L2 [36]. Two independent clustering algorithms identified TCF7L2 in a cluster containing JUNB, TEAD1, MEF2A, ELK4, and NKX3-1 (Fig. 5F, G). Interestingly, *MEF2A*, *TEAD1*, and *JUNB* were differentially expressed in low- *versus* high-efficiency TCF7L2-KD cells (Fig. 5H). Thus, a coordinated interaction between these three transcription factors might mediate the dose-dependent effects of TCF7L2-KD on adipogenesis. Finally, to identify TCF7L2 target genes driving the adipogenic phenotypes of TCF7L2-KD APs, we explored which genes from the curated adipogenesis 'hallmark' gene set [45] were differentially expressed between TCF7L2-KD and shCN cells. Approximately 60 % of genes (n = 113) from the above set were differentially expressed between near-total (n = 97) and/or partial (n = 63) TCF7L2-KD *versus* shCN APs of which 67 were non-overlapping (Table S2 & Fig. S13). Whilst this list is likely to include both direct and indirect TCF7L2 targets, some of the included genes (*e.g.*, ACLY, GPAM, GPX3, SLC25A1, and SCL27A1) were shown to harbor TCF7L2 binding sites within 1 kb of their promoters [15].

3.5. The T2D-risk allele at rs7903146 is associated with reduced AP TCF7L2 expression

Previous efforts to characterize the mechanism of action at *TCF7L2* revealed that the fine-mapped T2D-risk allele at rs7903146 overlaps enhancer histone marks in both islets and AT [46] (Fig. 6A). Whilst this variant was shown to be associated with increased islet *TCF7L2* expression [47], evidence demonstrating that it is associated with a *cis*-expression quantitative trait locus (eQTL) for *TCF7L2* in AT has been inconsistent [48,49]. By examining age-, BMI- and sex-adjusted *TCF7L2* mRNA abundance data from fractionated AT from up to 21 homozygous carriers of the T2D-risk variant (T) and 59 subjects homozygous for the wild-type allele (C) at rs7903146, we found that the T allele was associated with reduced *TCF7L2* expression in abdominal APs with a similar trend detected in gluteal APs (Fig. 6B, C). This finding was further substantiated in a subset of these samples by demonstrating lower TCF7L2 protein levels in abdominal APs derived from T *versus* C allele carriers (Fig. 6D). In cell-based luciferase assays, a 151 base pair nucleotide genomic sequence centred on rs7903146, exhibited allele-specific enhancer properties in abdominal APs and HEK293 cells with

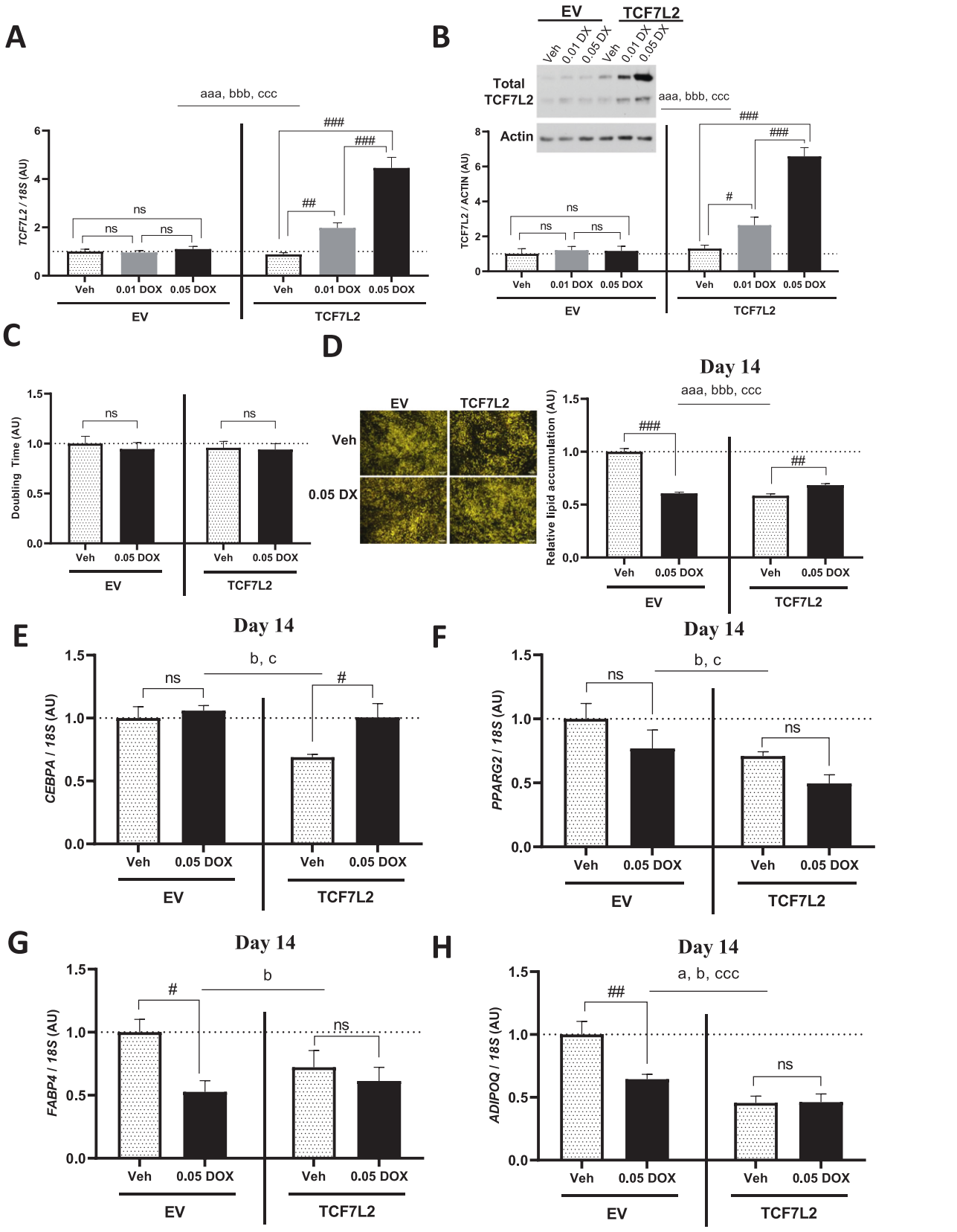

(caption on next page)

Fig. 3. Doxycycline-induced TCF7L2 over-expression in DFAT abdominal APs regulates adipogenesis. DFAT abdominal APs, stably transduced with the empty vector (EV) or TCF7L2 over-expression vector (TCF7L2), were cultured in the presence of vehicle (Veh) or DOX (final concentration: 0.01 μg/ml or 0.05 μg/ml) to induce TCF7L2 over-expression. TCF7L2 over-expression was confirmed by (A) qRT-PCR (two-way ANOVA, ^{aaa}Treatment * Genotype $P < 0.001$, ^{bbb}Treatment $P < 0.001$, ^{ccc}Genotype $P < 0.001$ followed by Šídák's multiple comparisons test) and (B) western blot in DFAT abdominal APs (two-way ANOVA, ^{aaa}Treatment * Genotype $P < 0.001$, ^{bbb}Treatment $P < 0.001$, ^{ccc}Genotype $P < 0.001$ followed by Šídák's multiple comparisons test). (C) Doubling time of DFAT abdominal APs (two-way ANOVA, Treatment * Genotype P = ns, Treatment P = ns, Genotype P = ns). (D) Representative micrographs of DFAT abdominal APs at day 14 of adipogenic differentiation (scale bar 100 μM). The histogram shows the relative lipid accumulation, assessed by AdipoRed lipid stain (n = 24 wells/group) (two-way ANOVA, ^{aaa}Treatment * Genotype $P < 0.001$, ^{bbb}Treatment $P < 0.001$, ^{ccc}Genotype $P < 0.001$ followed by Šídák's multiple comparisons test). (E–H) Relative mRNA levels of adipogenic genes *CEBPA* (two-way ANOVA, Treatment * Genotype p = ns, ^{b}Treatment $P < 0.05$, ^{c}Genotype $P < 0.05$ followed by Šídák's multiple comparisons test), *PPARG2* (two-way ANOVA, Treatment * Genotype P = ns, ^{b}Treatment $P < 0.05$, ^{c}Genotype $P < 0.05$ followed by Šídák's multiple comparisons test), *FABP4* (two-way ANOVA, Treatment * Genotype p = ns, ^{b}Treatment $P < 0.05$, Genotype p = ns followed by Šídák's multiple comparisons test) and *ADIPOQ* (two-way ANOVA, ^{a}Treatment * Genotype $P < 0.05$, ^{b}Treatment $P < 0.05$, ^{ccc}Genotype $P < 0.001$ followed by Šídák's multiple comparisons test) at day 14 of adipogenic differentiation. qRT-PCR data were normalized to 18S rRNA levels. Histograms are means ± SEM and expressed relative to vehicle treated EV cells (arbitrarily set to 1). Data obtained from 3 independent experiments. $^{###}P < 0.001$, $^{##}P < 0.01$, $^{#}P < 0.05$ (adjusted for multiple comparisons). Actin was used as western blot loading control.

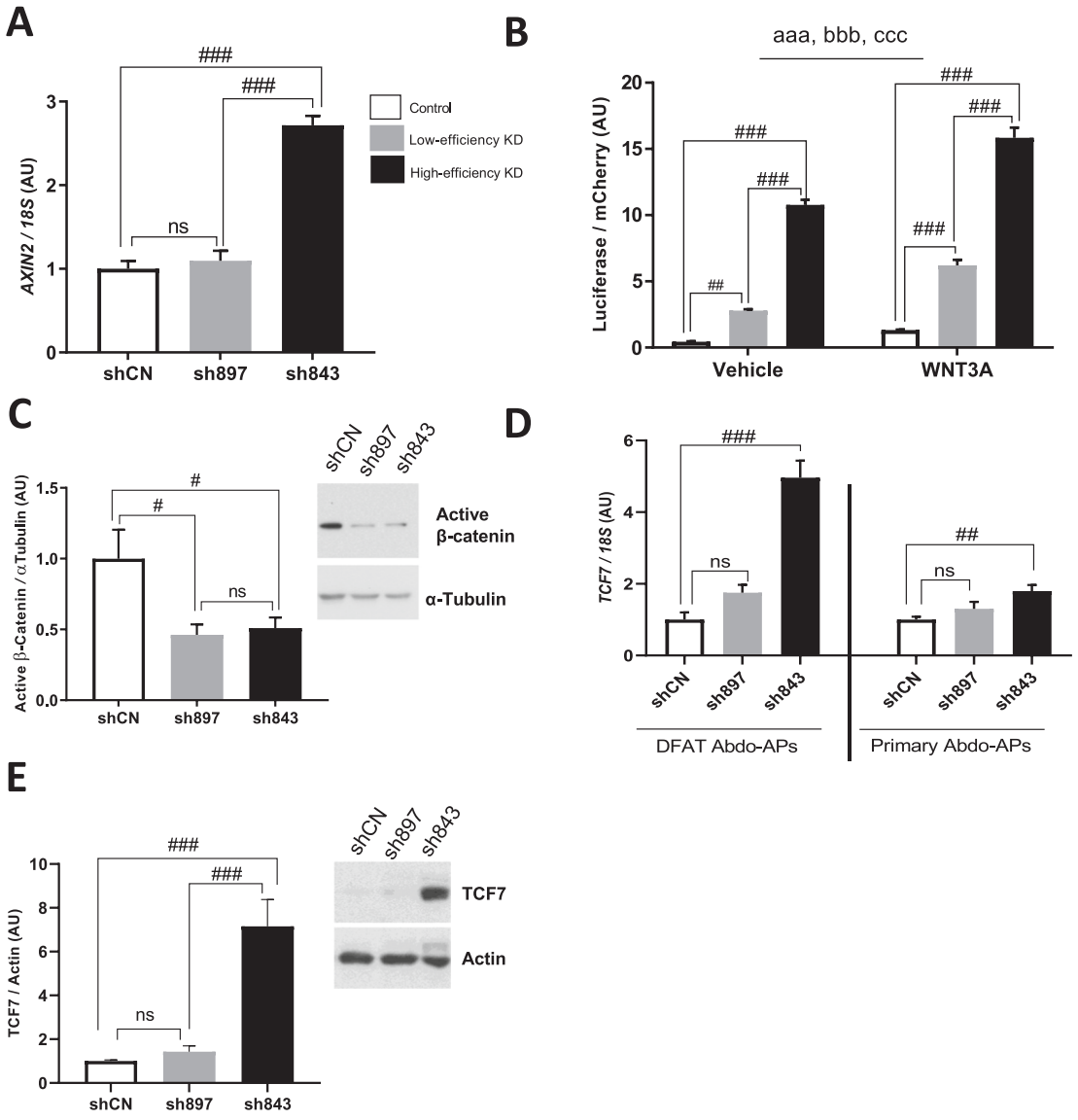

Fig. 4. TCF7L2 dose-dependently modulates WNT/β-catenin signaling. (A) *AXIN2* mRNA levels (one-way ANOVA followed by Tukey's multiple comparisons test), (B) TOPFlash promoter activity following 6 h treatment with vehicle (Veh) or 50 ng/ml WNT3A (n = 12 wells/group) (two-way ANOVA, ^{aaa}Treatment * Genotype p < 0.001, ^{bbb}Treatment $P < 0.001$, ^{ccc}Genotype $P < 0.001$ followed by Šídák's multiple comparisons test), (C) whole cell lysate active β-catenin protein levels (one-way ANOVA followed by Tukey's multiple comparisons test), and (D) *TCF7* mRNA levels following TCF7L2 KD in DFAT abdominal APs and primary abdominal APs (n = 2 subjects [0F]; mean age = 45.5. Mean BMI = 29.12; rs7903146 genotype [CC]). (One-way ANOVA followed by Tukey's multiple comparisons test.) (E) TCF7 protein levels in TCF7L2 KD DFAT abdominal APs (one-way ANOVA followed by Tukey's multiple comparisons test). shCN = scrambled control, sh897 = moderate and sh843 = high TCF7L2-KD DFAT abdominal APs. Actin was used as a loading control for western blots. qRT-PCR data were normalized to 18S rRNA levels. Histograms are means ± SEM. Data obtained from 3 independent experiments. $^{###}P < 0.001$, $^{##}P < 0.01$, $^{#}P < 0.05$ (adjusted for multiple comparisons).

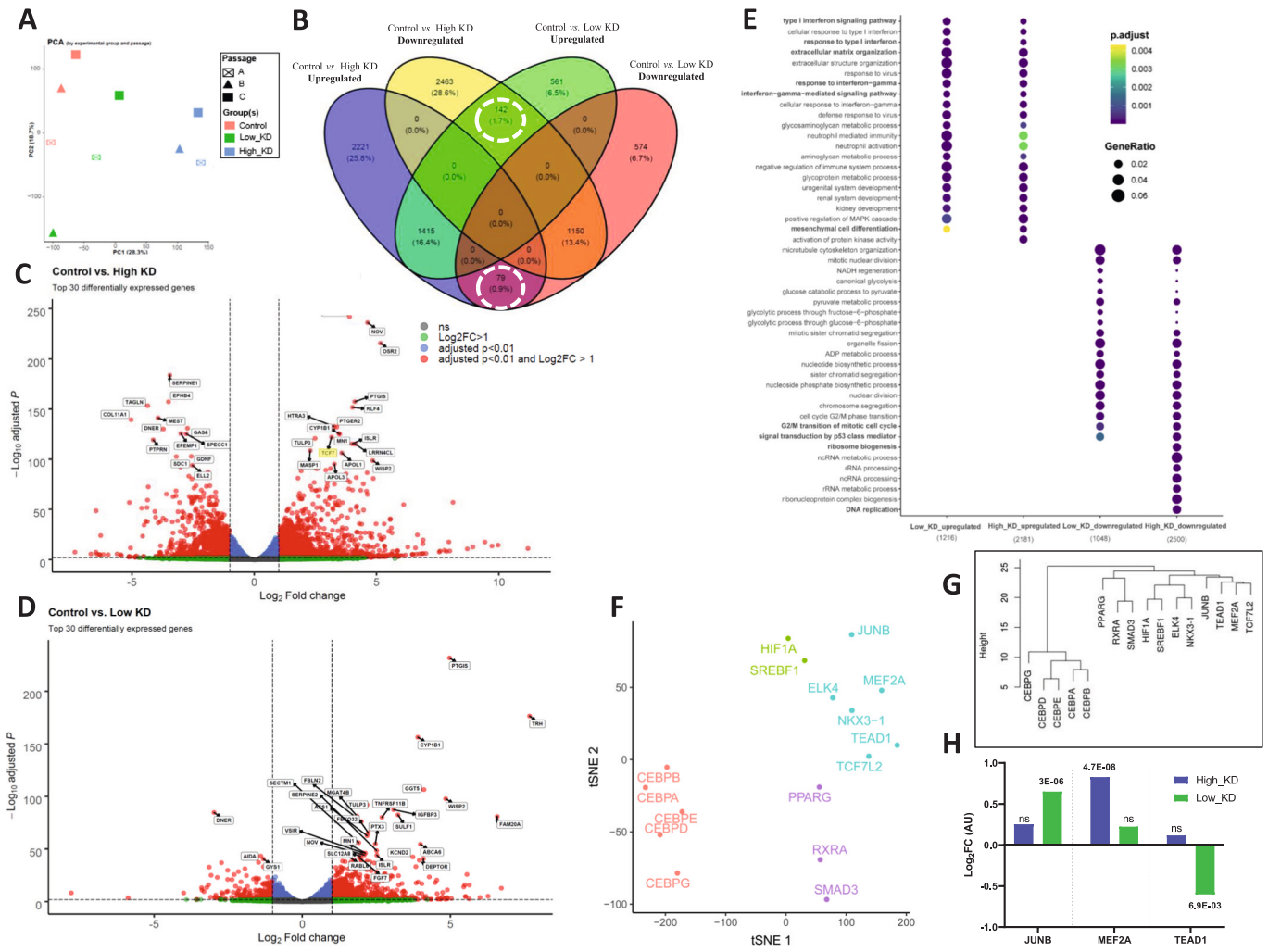

Fig. 5. Global transcriptional profiling reveals that TCF7L2 regulates multiple aspects of AP biology. (A) Principal component analysis (PCA) of the global transcriptomic profile of control (scrambled), moderate (sh897) and high-efficiency (sh843) TCF7L2-KD DFAT abdominal APs over 3 independent passages. (B) Venn diagram showing the overlap between differentially regulated genes from paired comparisons (FDR < 0.05). (C and D) Volcano plots showing the genes differentially regulated between control and (C) sh843 (*TCF7* was one of top 30 differentially regulated genes highlighted in yellow); or (D) sh897, TCF7L2-KD DFAT abdominal APs. Highlighted are the top 30 differentially regulated genes. (E) Overrepresentation analyses of genes differentially regulated in sh843 and sh897 DFAT abdominal APs, *vs.* controls in gene ontology biological processes gene sets. P-value was adjusted using the FDR (Benjamini-Hochberg) procedure. Gene ratio represents the percentage of total DEGs in the given GO term. (F) Dimensional reduction of transcription factors similarity by co-regulation of targets (see Supplementary methods). Colors represent high dimensional clustering by affinity propagation. (G) Dendrogram of transcription factors Euclidean distance. (H) *JUB*, *MEF2A* and *TEAD1* expression levels in high- and low-efficiency TCF7L2-KD cells (*vs.* scramble control) are shown. Padj is annotated for RNAseq $\log_2$ fold-change measurements. (For interpretation of the references to color in this figure legend, the reader is referred to the web version of this article.)

the T allele abolishing enhancer activity (Fig. 6E, F). However, attempts to generate clones, homozygous for the T and C variants at rs7903146 using genome editing, to investigate the effects of genotype at this single nucleotide variation (SNV) on *TCF7L2* expression in APs were unsuccessful (Fig. S14). Furthermore, histological assessment of abdominal AT biopsies from 19 age- and BMI-matched pairs of males homozygous either for the T or C allele at rs7903146 did not reveal any difference in median adipocyte size or adipocyte size distribution between the two genotypes (Fig. 6G, H). However, interrogation of plasma biochemistry data from 600 age- and BMI-matched OBB subject pairs showed that T2D-risk variant carriers had reduced AT insulin resistance [50], which was more pronounced in obese subjects (Fig. 6H, I). Finally, 48-hour, inducible TCF7L2-KD in differentiated adipocytes using sh843 (*i.e.*, the most efficient shRNA) did not influence basal or insulin-stimulated glucose uptake (Fig. S15). We conclude that genetic variation at rs7903146 might also influence T2D risk *via* effects on AP biology.

4. Discussion

Our study highlights a complex role for TCF7L2 in AP biology and AT function. We demonstrate that *TCF7L2* is broadly expressed in AT derived from different fat depots and that its transcript levels are reduced in abdominal AT in obesity. *TCF7L2* was also highly expressed in all adipose cell lineages examined, namely APs, mature adipocytes and endothelial cells with the former exhibiting the highest transcript levels. As such, it is likely to have pleiotropic roles in AT ranging from the regulation of AP biology to the modulation of mature adipocyte function and angiogenesis. Finally, higher BMI was paradoxically associated with elevated *TCF7L2* expression in isolated abdominal APs, despite reduced *TCF7L2* mRNA abundance in whole AT. Thus, obesity might lead to directionally opposite changes in *TCF7L2* expression in different AT cellular fractions.

To elucidate the role of TCF7L2 in AP biology, we undertook functional studies in immortalized and primary APs. These revealed that in abdominal APs TCF7L2-KD impairs proliferation and dose-dependently

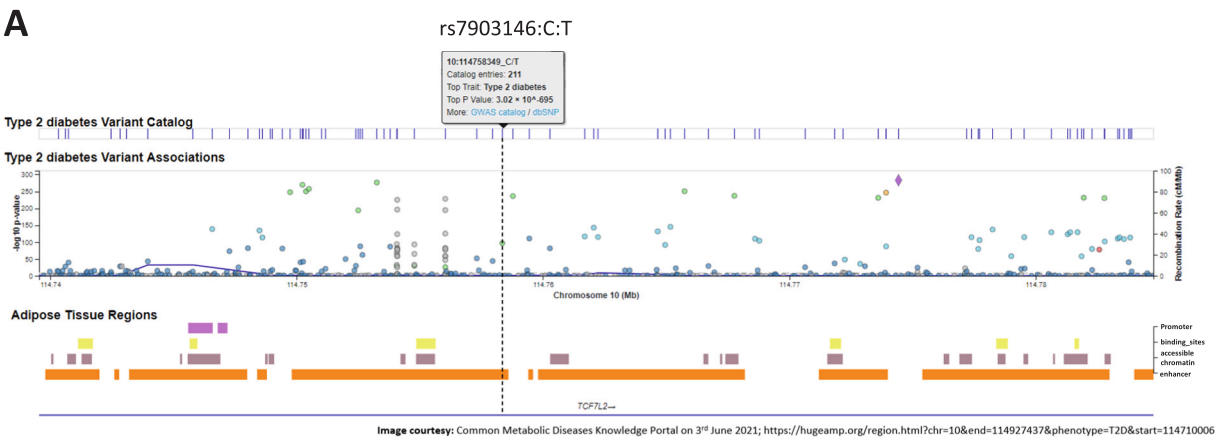

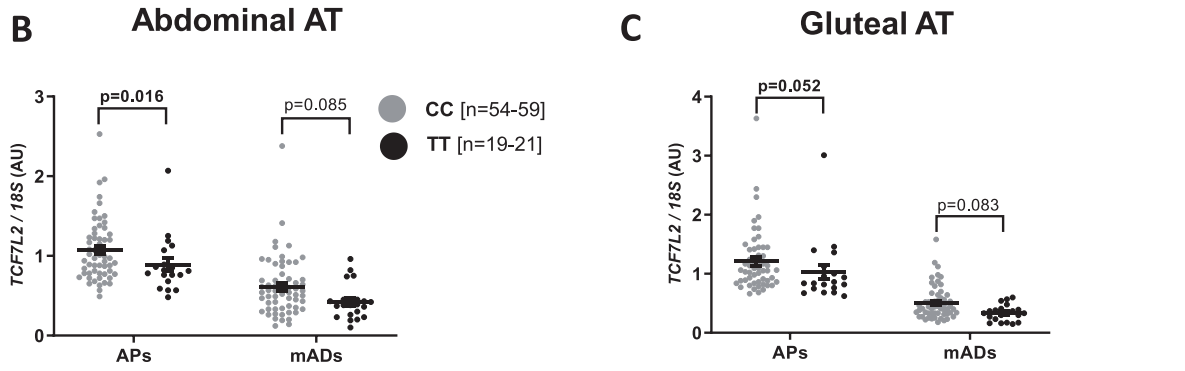

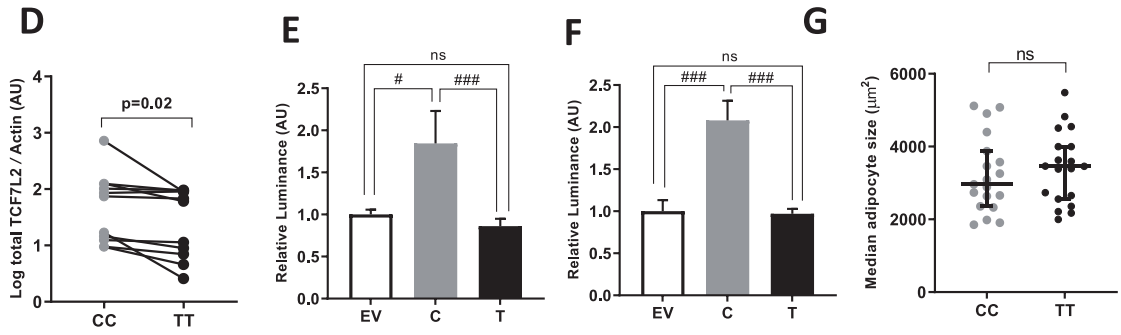

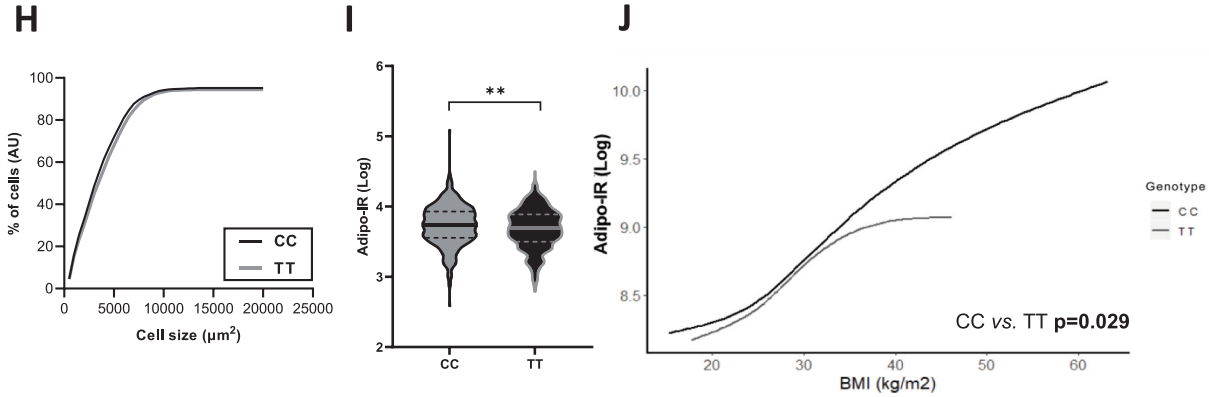

(caption on next page)

Fig. 6. The type 2 diabetes risk allele at rs7903146 reduces TCF7L2 expression in human abdominal APs. (A) Chromatin state map showing that rs7903146 overlaps an enhancer in AT. Orange – enhancer, grey – accessible chromatin, yellow – binding sites, pink – promoter (Image modified from Common Metabolic Diseases Knowledge Portal on 3rd June 2021; https://hugeamp.org/region.html?chr=10&end=114927437&phenotype=T2D&start=114710006). (B and C) *TCF7L2* expression in paired cultured APs and mature adipocytes (mADs) from SC (B) abdominal and (C) gluteal AT biopsies from homozygous carriers of the T2D allele T (n = 19–21 [4F]) *vs.* carriers of the non-risk allele C (n = 54–59 [29F]). TT carriers, age - 42.8 ± 6.4 years, BMI - 26.2 ± 6.0 kg/m^2. CC carriers, age - 45.8 ± 9.5 years, BMI - 27.3 ± 3.8 kg/m^2. Data analysed by (General Linear Model) univariate analysis using *TCF7L2* mRNA levels as dependent variable, genotype as fixed variable and age, BMI and gender as covariate(s). (D) TCF7L2 protein levels in cultured abdominal APs from age-, BMI- and sex-matched homozygous carriers of the T2D risk allele T *vs.* carriers of the non-risk allele C (n = 11/group) (paired *t*-test). Actin was used as western blot loading control. (E and F) Luciferase reporter assay in (E) DFAT abdominal APs and (F) HEK293 cells transfected with empty vector (EV) or the luciferase reporter vector containing 151 bp genomic sequence centred on the T2D risk allele T or the non-risk allele C (n = 12–16 replicates/group) (Kruskal-Wallis test followed by Dunn's multiple comparisons test). $^{\#\#\#}P < 0.001$, $^{\#}P < 0.05$ (adjusted for multiple comparisons). (G) Median adipocyte area (μm^2) (paired t-test) and (H) cumulative frequency distribution of median adipocyte area (μm^2) calculated from the histological sections of abdominal AT from 19 pairs of age- and BMI-matched males grouped by rs7903146 genotype. CC carriers, age - 44.2 ± 6.3 years, BMI - 25.4 ± 2.8 kg/m^2. TT carriers, age - 44.1 ± 7.3 years, BMI - 25.1 ± 2.7 kg/m^2. Error bars are median with 95 % CI. (I) Comparison of adipose tissue insulin resistance (adipo-IR = Fasting Insulin * FFAs) between age-, BMI- and sex-matched homozygous carriers of the T2D risk allele (T) and the non-risk allele (C) (n = 600 pairs) (Wilcoxon matched-pairs signed rank test). Violin plot including medians (solid line) and quartiles (broken lines) are shown. (J) Generalized additive models was used to compare the slopes of adipo-IR (logged) against BMI and smoothing was done for each genotype separately. Smoothened splines showing the relationship between adipo-IR and BMI for homozygous carriers of the T2D risk allele (T) and carriers of the non-risk allele (C) at rs7903146. $^{**}P < 0.01$. See Supplementary Table S2 for anthropometric and plasma biochemistry data for (I and J). (For interpretation of the references to color in this figure legend, the reader is referred to the web version of this article.)

modulates adipogenesis. We speculate that the primary role of TCF7L2 in these cells is to promote their maintenance and/or expansion and to restrain adipogenesis since only near-total TCF7L2-KD led to impaired adipocyte differentiation. In contrast, partial TCF7L2-KD promoted adipogenesis in both DFAT and primary abdominal APs. TCF7L2-KD in gluteal APs also dose-dependently modulated adipogenesis. However, in marked contrast to findings in abdominal cells, near-total TCF7L2-KD in gluteal APs led to enhanced adipocyte differentiation. Interestingly, adipocyte specific TCF7L2 deletion in mice was also shown to regulate fat cell size and AT mass in a depot-specific manner [15]. Collectively, these findings reconcile the discrepant adipogenic effects of TCF7L2 KD and knockout in 3T3-L1 preadipocytes and inguinal mouse APs respectively reported in previous studies [14,15]. Furthermore, they suggest that abdominal APs express a distinct complement of *TCF7L2* splice variants and/or a different set of TCF7L2 interacting transcriptional co-regulators than gluteal APs. We also investigated the effects of dose-dependent over-expression of TCF7L2 on abdominal AP function using an inducible Tet-On system to tightly titrate ectopic TCF7L2 protein production. In these experiments, 2-fold TCF7L2 over-expression was not sustained throughout adipogenesis whilst 2-week treatment with higher dose doxycycline (driving 5-fold TCF7L2 over-expression) appeared to suppress adipogenesis in both empty vector and TCF7L2 over-expressing APs. Despite these limitations, these studies produced broadly complementary results with the KD experiments in demonstrating that 2-fold TCF7L2 over-expression tended to inhibit lipid accumulation whilst 5-fold over-expression accelerated adipogenesis.

To decipher the signaling pathways mediating the actions of TCF7L2 in abdominal AP biology, we examined canonical WNT signaling in TCF7L2-KD cells. These experiments revealed that in abdominal APs TCF7L2 functions to inhibit WNT pathway activity. Whilst *prima facie* paradoxical, this result is consistent with previous findings in TCF7L2-KD 3T3-L1 cells [14]. Tang et al. also showed that TCF7L2 displayed a cell-type specific activity to both enhance and inhibit WNT signaling [51]. The transcriptional repressive ability of TCF7L2 seems to track to its carboxyl terminus, which contains binding motifs for the C-terminal binding protein (CtBP) transcriptional repressors. Additionally, or alternatively, small repressor-recruiting motifs in the central region of the protein might be involved, including an interaction domain for Groucho/TLE family members such as TLE3, which was shown to antagonize the activation of TCF7L2 by β-catenin in preadipocytes [8,10,51–53]. These regions are only present in some *TCF7L2* splice variants. WNT/β-catenin signaling functions to inhibit adipogenesis [12]. Accordingly, high-efficiency TCF7L2-KD in abdominal APs resulted in impaired adipocyte differentiation concomitant with canonical WNT signaling activation. However, down-regulation of TCF7L2 expression within a more physiological range in the same cells led to increased adipogenesis despite mild WNT/β-catenin pathway activation. These data suggest that TCF7L2 might engage multiple signaling pathways to influence abdominal AP biology. Alternatively, WNT signaling might have dose-dependent effects on adipogenesis, with mild activation insufficient to block early differentiation whilst promoting lipid accumulation *via de novo* lipogenesis during the latter stages of adipogenesis [28,54–56]. Indeed, we were unable to rescue the diminished lipid accumulation in high-efficiency TCF7L2-KD cells with continuous treatment during differentiation with a small molecule (KYA1797K) β-catenin antagonist. Transient TCF7-KD also failed to rescue differentiation of these cells. It would be interesting to determine whether stable TCF7-KD or, given the functional redundancy among TCF/LEF factors in the transcription of β-catenin targets, over-expression of dominant negative TCF7L2 can restore adipogenesis in high-efficiency TCF7L2-KD cells.

To elucidate the genes, pathways and biological processes regulated by TCF7L2 in APs, we undertook genome-wide transcriptional profiling of abdominal TCF7L2-KD cells. Consistent with our functional studies, these experiments showed that TCF7L2-KD activates transcriptional programs, which inhibit proliferation and modulate mesenchymal cell differentiation. Furthermore, they revealed that TCF7L2 might also regulate many other aspects of AP biology including ECM remodeling, immune and inflammatory signaling, and potentially apoptosis and/or senescence. These findings expand the potential functional repertoire of TCF7L2 in AT. The RNA sequencing experiments also revealed that high-efficiency TCF7L2-KD in APs suppressed gene expression programs associated with enhanced canonical WNT signaling. How can we reconcile this finding with the results of the *in vitro* WNT/β-catenin signaling studies? Firstly, APs express several *TCF7L2* splice variants functioning to both repress and activate WNT target genes [48,58] with the former isoforms probably constituting the majority in abdominal APs. Secondly, in near-total TCF7L2-KD cells expression of *TCF7*, a TCF7L2 target gene [59], was up-regulated. Given that TCF/LEF family members display partially overlapping DNA binding patterns [60] and functional redundancy [8], we speculate that increased TCF7 abundance drove, at least partly, the higher β-catenin transcriptional activity detected in promoter reporter assays in near-total TCF7L2-KD cells. However, because TCF7 cannot compensate for the absence of TCF7L2 at many WNT target gene promoters, AP TCF7L2-KD led to down-regulation of several classic WNT target genes and pathways. This paradigm has been reported in other cell types [61,62]. For example, in the kidney, WNT/β-catenin signaling dose-dependently modulated nephron progenitor cell fate, with low activation promoting cell maintenance and expansion and more robust activation stimulating nephrogenic differentiation. Interestingly, this switch involved an exchange from inhibitory TCF7L1/TCF7L2 to activating TCF7/LEF1 complexes at the enhancers of differentiation promoting target genes consequent to rising β-catenin levels [61]. Finally, whilst based on our findings the

impaired adipogenic capacity of high-efficiency TCF7L2-KD cells is unlikely to be driven by enhanced interferon-JAK/STAT signaling, we do highlight possible roles for the anti-adipogenic transcription factors JUNB, TEAD1, and MEF2A [43], in mediating this link. Interestingly, members of the AP1 family, including JUNB, were shown to interact with β-catenin and TCF7L2 physically and functionally to regulate gene expression and intestinal cancer development [63,64]. Furthermore, bioinformatic analysis of genomic regions bound by TCF7L2 in differentiated inguinal APs, revealed that the most enriched non-TCF7L2 motif was that of JUNB [15].

GWAS meta-analyses have identified associations between eight independent signals at *TCF7L2* and T2D susceptibility [23]. At least three of these overlap active chromatin regions in AT [23] although, only rs7903146 has received attention to date. It has been demonstrated through analysis of GWAS metadata of T2D-related traits [65,66] and human physiological studies [67] that the risk allele at this SNV increases T2D susceptibility *via* impaired insulin secretion. Additionally, this variant was shown colocalize with a *cis*-eQTL for *TCF7L2* in pancreatic islets [68] and to be associated with increased *TCF7L2* expression in islets and β-cells [47,69,70]. These data have established that rs7903146 increases T2D risk primarily through islet dysfunction, which is probably driven by increased *TCF7L2* expression in beta cells. Nevertheless, this SNV may also influence T2D predisposition *via* actions in adipose cells as it was shown to overlap active enhancer histone marks in AT [46] and to be associated with fat distribution [24]. Using a "soft clustering" approach to group variant-trait associations ascertained from GWAS for 94 independent T2D signals and 47 diabetes-related traits, another study also provided suggestive evidence that "lipodystrophy-like" insulin resistance might contribute to T2D predisposition at rs7903146 [66]. Extending these findings, we now demonstrate that rs7903146 is an eQTL for *TCF7L2* in abdominal APs with the T allele *reducing TCF7L2* expression. Furthermore, we corroborated these data by demonstrating that the T2D-risk variant at this SNV was associated with reduced AP TCF7L2 protein levels and displayed allele-specific enhancer activity, which was directionally consistent with the eQTL data in luciferase assays. Nonetheless, these results should be interpreted with caution as we were unable to generate edited clones to investigate the effects of rs7903146 genotype on *TCF7L2* expression in APs. Interestingly rs7903146 confers higher T2D susceptibility in lean *versus* obese subjects [71]. Our results might offer a partial explanation for this paradox. In our study population the T2D-risk variant at this SNV was associated with enhanced AT insulin sensitivity, which was more pronounced in obese subjects. Whilst we detected no difference in adipocyte size based on rs7903146 genotype, our study sample (n = 19) comprised only one pair of obese subjects due to limited numbers of homozygous obese, T2D-risk allele carriers in the OBB (Fig. 6I). Based on the dose-dependent effects of TCF7L2 on adipogenesis demonstrated herein, it would be interesting to determine whether the T2D-predisposing allele at rs7903146 is associated with differential effects on adipocyte size in lean *versus* obese subjects; with smaller fat cells, indicative of enhanced adipogenesis, specifically seen in obese individuals, who displayed higher baseline AP *TCF7L2* expression (Fig. 7).

Our study has several strengths. These include access to fractionated and/or whole AT derived from many volunteers with a wide BMI range and from multiple fat depots. Further strengths are the use of primary and immortalized human abdominal (and gluteal) APs in functional studies and the provision of multiple, independent lines of evidence to substantiate the dose-dependent actions of TCF7L2 on adipogenesis. Finally, we were able to investigate the associations between rs7903146 and AT morphology, as well as *TCF7L2* expression in whole and fractionated AT using a recruitment by genotype approach from the OBB, a cohort comprising over 7000 healthy volunteers with available genotype, anthropometry, and fasting biochemistry data. Limitations include the lack of identification of a mechanism(s) for the adipogenic effects of TCF7L2. Additionally, we did not corroborate the association between rs7903146 and *TCF7L2* expression in abdominal APs in an independent cohort nor substantiated this finding using genome editing.

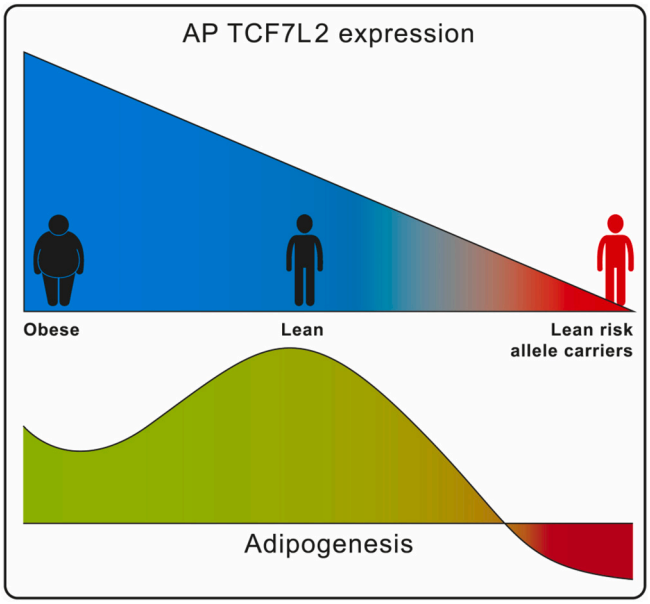

Fig. 7. Schematic summarizing the role of TCF7L2 and impact of rs7903146 genotype on human AP biology. TCF7L2 has dose-dependent effects on adipogenesis with moderate and high-efficiency knockdown leading to enhanced and impaired adipogenesis respectively *in vitro*. In fractionated adipose tissue expression of *TCF7L2* in APs correlates positively with donor BMI whilst the T2D risk variant (T) at rs7903146 is associated with reduced AP TCF7L2 expression. Based on these findings we speculate that lean homozygous T2D risk variant carriers would have the lowest AP TCF7L2 expression and consequently impaired adipogenesis, larger adipocytes, increased adipo-IR and higher susceptibility to T2D compared with obese T2D risk variant carriers.

In summary, we highlight an important but complex role of TCF7L2 in AP biology with both dose- and depot-dependent effects on adipogenesis. We also demonstrate that rs7903146 is associated with reduced TCF7L2 expression in abdominal APs and hence might have *cis*-regulatory effects outside the pancreas. Thus, in addition to islet dysfunction, altered AP function consequent to changes in *TCF7L2* expression might also influence the T2D predisposition conferred by this SNV. Collectively, our results suggest that targeting TCF7L2 expression and/or activity in AT might hold therapeutic potential for the management of T2D and associated metabolic disorders. To aid these translational efforts, future studies should define the role of TCF7L2 in human adipose cells derived from different fat depots and characterize the impact of T2D-associated regulatory variants at *TCF7L2*, which overlap open chromatin in adipose cells on adipose *TCF7L2* expression and AT function.

Supplementary data to this article can be found online at https://doi.org/10.1016/j.metabol.2022.155240.

CRediT authorship contribution statement

Manu Verma: Methodology, Investigation, Writing – original draft, Writing – review & editing. **Nellie Y. Loh:** Methodology, Investigation, Writing – review & editing. **Rugivan Sabaratnam:** Investigation, Writing – review & editing. **Senthil K. Vasan:** Methodology, Investigation, Writing – review & editing. **Andrea D. van Dam:** Investigation, Writing – review & editing. **Marijana Todorčević:** Investigation, Writing – review & editing. **Matthew J. Neville:** Investigation, Writing – review & editing. **Enrique Toledo:** Writing – review & editing. **Fredrik Karpe:** Writing – review & editing, Funding acquisition, Resources, Supervision. **Constantinos Christodoulides:** Conceptualization, Investigation, Writing – original draft, Writing – review & editing, Funding acquisition, Resources, Supervision.

Declaration of competing interest

The authors declare that there is no duality of interest associated with this manuscript. MV and ADVD were supported by Novo Nordisk Postdoctoral Fellowships. The funders had no role in study design, analysis or reporting of the current work. Currently, MV and ENT are employees of Novo Nordisk Ltd., UK (Novo Nordisk Research Centre, Oxford).

Acknowledgements

We thank the volunteers from the OBB (www.oxfordbiobank.org.uk) for their participation in this study and the nurses at the Clinical Research Unit for their help in recruitment and sample collection from OBB volunteers.

Funding

CC (FS/16/45/32359) and FK (RG/17/1/32663) are funded by the British Heart Foundation. MV and ADVD were supported by Novo Nordisk Postdoctoral Fellowships run in partnership with the University of Oxford. The OBB and Oxford BioResource are funded by the NIHR Oxford Biomedical Research Centre.

Data availability

All data and materials are available from the corresponding author upon reasonable request.

References

[1] Mann JP, Savage DB. What lipodystrophies teach us about the metabolic syndrome. J Clin Investig 2019;129:4009–21.
[2] Kahn CR, Wang G, Lee KY. Altered adipose tissue and adipocyte function in the pathogenesis of metabolic syndrome. J Clin Investig 2019;129:3990–4000.
[3] Sun K, Tordjman J, Clément K, Scherer PE. Fibrosis and adipose tissue dysfunction. Cell Metab 2013;18:470–7.
[4] Marcelin G, Silveira ALM, Martins LB, Ferreira AVM, Clément K. Deciphering the cellular interplays underlying obesity-induced adipose tissue fibrosis. J Clin Investig 2019;129:4032–40.
[5] Christodoulides C, Lagathu C, Sethi JK, Vidal-Puig A. Adipogenesis and WNT signalling. Trends Endocrinol Metab 2009;20:16–24.
[6] Nusse R, Clevers H. Wnt/β-catenin signaling, disease, and emerging therapeutic modalities. Cell 2017;169:985–99.
[7] Bagchi DP, MacDougald OA. Wnt signaling: from mesenchymal cell fate to lipogenesis and other mature adipocyte functions. Diabetes 2021;70:1419–30.
[8] Cadigan KM, Waterman ML. TCF/LEFs and wnt signaling in the nucleus. Cold Spring Harb Perspect Biol 2012;4:1–22.
[9] Aguet F, et al. Genetic effects on gene expression across human tissues. Nature 2017;550:204–13.
[10] Mao CD, Byers SW. Cell-context dependent TCF/LEF expression and function: alternative tales of repression, de-repression and activation potentials. Crit Rev Eukaryot Gene Expr 2011;21:207–36.
[11] Lien WH, Fuchs E. Wnt some lose some: transcriptional governance of stem cells by Wnt/β-catenin signaling. Genes Dev 2014;28:1517–32.
[12] Ross SE, et al. Inhibition of adipogenesis by wnt signaling. Science 2000;1979 (289):950–3.
[13] Kennell JA, O'Leary EE, Gummow BM, Hammer GD, MacDougald OA. T-cell factor 4N (TCF-4N), a novel isoform of mouse TCF-4, synergizes with β-catenin to coactivate C/EBPα and steroidogenic factor 1 transcription factors. Mol Cell Biol 2003;23:5366–75.
[14] Chen X, et al. The diabetes gene and wnt pathway effector TCF7L2 regulates adipocyte development and function. Diabetes 2018;67:554–68.
[15] Geoghegan G, et al. Targeted deletion of Tcf7l2 in adipocytes promotes adipocyte hypertrophy and impaired glucose metabolism. Mol Metab 2019;24:44–63.
[16] Chen ZL, et al. Acute wnt pathway activation positively regulates leptin gene expression in mature adipocytes. Cell Signal 2015;27:587–97.
[17] Yang H, Li Q, Lee JH, Shu Y. Reduction in Tcf7l2 expression decreases diabetic susceptibility in mice. Int J Biol Sci 2012;8:791–801.
[18] Savic D, et al. Alterations in TCF7L2 expression define its role as a key regulator of glucose metabolism. Genome Res 2011;21:1417–25.
[19] Bailey KA, et al. Evidence of non-pancreatic beta cell-dependent roles of Tcf7l2 in the regulation of glucose metabolism in mice. Hum Mol Genet 2015;24:1646–54.
[20] Nguyen-Tu MS, Martinez-Sanchez A, Leclerc I, Rutter GA, da Silva Xavier G. Adipocyte-specific deletion of Tcf7l2 induces dysregulated lipid metabolism and impairs glucose tolerance in mice. Diabetologia 2021;64:129–41.
[21] Karczewska-Kupczewska M, Stefanowicz M, Matulewicz N, Nikołajuk A, Straczkowski M. Wnt signaling genes in adipose tissue and skeletal muscle of humans with different degrees of insulin sensitivity. J Clin Endocrinol Metabol 2016;101:3079–87.
[22] Cauchi S, et al. TCF7L2 is reproducibly associated with type 2 diabetes in various ethnic groups: a global meta-analysis. J Mol Med 2007;85:777–82.
[23] Mahajan A, et al. Fine-mapping type 2 diabetes loci to single-variant resolution using high-density imputation and islet-specific epigenome maps. Nat Genet 2018; 50:1505–13.
[24] Pulit SL, et al. Meta-Analysis of genome-wide association studies for body fat distribution in 694 649 individuals of European ancestry. Hum Mol Genet 2019;28: 166–74.
[25] Lu J, Varghese RT, Zhou L, Vella A, Jensen MD. Glucose tolerance and free fatty acid metabolism in adults with variations in TCF7L2 rs7903146. Metab Clin Exp 2017;68:55–63.
[26] Karpe F, et al. Cohort profile: the Oxford Biobank. Int J Epidemiol 2018;47. 21-21g.
[27] Loh NY, et al. RSPO3 impacts body fat distribution and regulates adipose cell biology in vitro. Nat Commun 2020;11.
[28] Loh NY, et al. LRP5 regulates human body fat distribution by modulating adipose progenitor biology in a dose- and depot-specific fashion. Cell Metab 2015;21: 262–72.
[29] Todorčević M, et al. A cellular model for the investigation of depot specific human adipocyte biology. Adipocyte 2017;6:40–55.
[30] Fuerer C, Nusse R. Lentiviral vectors to probe and manipulate the Wnt signaling pathway. PLoS ONE 2010;5.
[31] Tetsu O, McCormick F. β-catenin regulates expression of cyclin D1 in colon carcinoma cells. Nature 1999;398:422–6.
[32] Wiederschain D, et al. Single-vector inducible lentiviral RNAi system for oncology target validation. Cell Cycle 2009;8:498–504.
[33] Chen S, et al. Genome-wide CRISPR screen in a mouse model of tumor growth and metastasis. Cell 2015;160:1246–60.
[34] Brinkman EK, Chen T, Amendola M, van Steensel B. Easy quantitative assessment of genome editing by sequence trace decomposition. Nucleic Acids Res 2014;42.
[35] Yu G, Wang LG, Han Y, He QY. ClusterProfiler: an R package for comparing biological themes among gene clusters. OMICS 2012;16:284–7.
[36] Toledo EM, et al. Srebf1 controls midbrain dopaminergic neurogenesis. Cell Rep 2020;31.
[37] Merrick D, et al. Identification of a mesenchymal progenitor cell hierarchy in adipose tissue. Science 2019;1979(364):1–25.
[38] Vijay J, et al. Single-cell analysis of human adipose tissue identifies depot- and disease-specific cell types. Nat Metab 2019. https://doi.org/10.1038/s42255-019-0152-6.
[39] Cha PH, et al. Small-molecule binding of the axin RGS domain promotes β-catenin and Ras degradation. Nat Chem Biol 2016;12:593–600.
[40] Madan B, et al. Temporal dynamics of Wnt-dependent transcriptome reveals an oncogenic Wnt / MYC / ribosome axis Graphical abstract Find the latest version. J Clin Investig 2018;128:5620–33.
[41] Lee K, Um SH, Rhee DK, Pyo S. Interferon-alpha inhibits adipogenesis via regulation of JAK/STAT1 signaling. Biochim Biophys Acta Gen Subj 2016;1860: 2416–27.
[42] McGillicuddy FC, et al. Interferon γ attenuates insulin signaling, lipid storage, and differentiation in human adipocytes via activation of the JAK/STAT pathway. J Biol Chem 2009;284:31936–44.
[43] Rauch A, et al. Osteogenesis depends on commissioning of a network of stem cell transcription factors that act as repressors of adipogenesis. Nat Genet 2019;51: 716–27.
[44] Rosen ED, Walkey CJ, Puigserver P, Spiegelman BM. Transcriptional regulation of adipogenesis. www.genesdev.org; 2000.
[45] Liberzon A, et al. The molecular signatures database hallmark gene set collection. Cell Syst 2015;1:417–25.
[46] Varshney A, et al. Genetic regulatory signatures underlying islet gene expression and type 2 diabetes. Proc Natl Acad Sci U S A 2017;114:2301–6.
[47] Viñuela A, et al. Genetic variant effects on gene expression in human pancreatic islets and their implications for T2D. Nat Commun 2020;11.
[48] Mondal AK, et al. Genotype and tissue-specific effects on alternative splicing of the transcription factor 7-like 2 gene in humans. J Clin Endocrinol Metabol 2010;95: 1450–7.
[49] Prokunina-Olsson L, Kaplan LM, Schadt EE, Collins FS. Alternative splicing of TCF7L2 gene in omental and subcutaneous adipose tissue and risk of type 2 diabetes. PLoS ONE 2009;4:1–8.
[50] Søndergaard E, de Ycaza AEE, Morgan-Bathke M, Jensen MD. How to measure adipose tissue insulin sensitivity. J Clin Endocrinol Metabol 2017;102:1193–9.
[51] Tang W, et al. A genome-wide RNAi screen for Wnt/β-catenin pathway components identifies unexpected roles for TCF transcription factors in cancer. Proc Natl Acad Sci U S A 2008;105:9697–702.
[52] Villanueva CJ, et al. TLE3 is a dual-function transcriptional coregulator of adipogenesis. Cell Metab 2011;13:413–27.
[53] Young RM, et al. Developmentally regulated Tcf7l2 splice variants mediate transcriptional repressor functions during eye formation. Elife 2019;8:1–24.
[54] Basham KJ, et al. A ZNRF3-dependent Wnt/β-catenin signaling gradient is required for adrenal homeostasis. Genes Dev 2019;33:209–20.
[55] Bagchi DP, et al. Wntless regulates lipogenic gene expression in adipocytes and protects against diet-induced metabolic dysfunction. Mol Metab 2020;39.
[56] Bagchi DP, et al. Wnt/β-catenin signaling regulates adipose tissue lipogenesis and adipocyte-specific loss is rigorously defended by neighboring stromal-vascular cells. Mol Metab 2020;42.

[58] Kaminska D, et al. Adipose tissue TCF7L2 Splicing is regulated by weight loss and associates with glucose and fatty acid metabolism. Diabetes 2012;61:2807–13.
[59] Hatzis P, et al. Genome-wide pattern of TCF7L2/TCF4 chromatin occupancy in colorectal cancer cells. Mol Cell Biol 2008;28:2732–44.
[60] Schuijers J, Mokry M, Hatzis P, Cuppen E, Clevers H. Wnt-induced transcriptional activation is exclusively mediated by TCF/LEF. EMBO J 2014;33:146–56.
[61] Guo Q, et al. A β-catenin-driven switch in tcf/lef transcription factor binding to dna target sites promotes commitment of mammalian nephron progenitor cells. elife 2021;10:1–47.
[62] Lien WH, et al. In vivo transcriptional governance of hair follicle stem cells by canonical Wnt regulators. Nat Cell Biol 2014;16:179–90.
[63] Toualbi K, et al. Physical and functional cooperation between AP-1 and β-catenin for the regulation of TCF-dependent genes. Oncogene 2007;26:3492–502.
[64] Nateri AS, Spencer-Dene B, Behrens A. Interaction of phosphorylated c-Jun with TCF4 regulates intestinal cancer development. Nature 2005;437:281–5.
[65] Mahajan A, et al. Refining the accuracy of validated target identification through coding variant fine-mapping in type 2 diabetes article. Nat Genet 2018;50:559–71.
[66] Udler MS, et al. Type 2 diabetes genetic loci informed by multi-trait associations point to disease mechanisms and subtypes: a soft clustering analysis. PLoS Med 2018;15:1–23.
[67] Ingelsson E, et al. Detailed physiologic characterization reveals diverse mechanisms for novel genetic loci regulating glucose and insulin metabolism in humans. Diabetes 2010;59:1266–75.
[68] Mahajan A, et al. Multi-ancestry genetic study of type 2 diabetes highlights the power of diverse populations for discovery and translation. Nat Genet 2022;54:560–72.
[69] Lyssenko V, et al. Mechanisms by which common variants in the TCF7L2 gene increase risk of type 2 diabetes. J Clin Invest 2007;117:2155–63.
[70] Miguel-Escalada I, et al. Human pancreatic islet three-dimensional chromatin architecture provides insights into the genetics of type 2 diabetes. Nat Genet 2019;51.
[71] Cauchi S, Nead KT, Choquet H, Horber F, Potoczna N, Balkau B, Marre M, Charpentier G, Froguel P, Meyre D. The genetic susceptibility to type 2 diabetes may be modulated by obesity status: implications for association studies. BMC Med. Genet. 2008;9(45). https://doi.org/10.1186/1471-2350-9-45. PMID: 18498634 PMCID: PMC2412856.